AIP Applied Physics Letters

Electrical conduction of buried SiO 2 layers analyzed by photon stimulated electron tunneling

V. V. Afanas’ev and A. Stesmans

Citation: Applied Physics Letters **70**, 1260 (1997); doi: 10.1063/1.118546
View online: http://dx.doi.org/10.1063/1.118546
View Table of Contents: http://scitation.aip.org/content/aip/journal/apl/70/10?ver=pdfcov
Published by the AIP Publishing

Electrical conduction of buried SiO_2 layers analyzed by photon stimulated electron tunneling

V. V. Afanas'ev[a] and A. Stesmans
Department of Physics, University of Leuven, Celestijnenlaan 200D, 3001 Leuven, Belgium

(Received 29 October 1996; accepted for publication 3 January 1997)

The conductivity of buried SiO_2 layers produced by implantation of oxygen ions into silicon was compared with the photon stimulated electron tunneling from Si into SiO_2. The latter process is found to originate from defects located in interfacial SiO_2 layers with an electron energy level 2.8 eV below the oxide conduction band. The dark and photon induced currents show a correlated dependence on the electric field strength in the oxide, and both increase with the Si enrichment of the oxide, thus advancing the isolated defects as the common origin of both currents. The same defects were also observed in thermally grown and deposited oxides, so they appear as intrinsic imperfections related to the excess silicon in SiO_2. *© 1997 American Institute of Physics.* [S0003-6951(97)00110-1]

Silicon-on-insulator structures fabricated using the separation-by-implantation-of-oxygen (SIMOX) technique are of particular interest for advanced electronic devices because of excellent thickness uniformity of the top Si layer.[1] However, they suffer from substantially enhanced electrical conduction of the buried oxide (BOX) layer as compared to the superb thermally grown SiO_2 on Si.[2,3] The BOX conduction has two components: First, there is the low field conduction related to the localized shorts between the top Si and Si substrate. These imperfections are usually ascribed to particulate contamination of the Si wafer during oxygen implantation resulting in formation of ''Si pipes'' in the BOX.[2] Over the last few years this localized conductance has been significantly reduced both by eliminating the particulate contaminants,[4] and by finding ways to oxidize the Si pipes.[5–7] Second, there is the high field conductance of BOX which manifests itself as a reduced barrier for electron tunneling at the Si/BOX interface.[3] This conduction is also ascribed to the presence of excess Si in the BOX, but cannot be completely eliminated either by supplemental implantation of oxygen into the BOX[3,5] or by reoxidation of the BOX with[6] or without top Si.[3] The origin of the barrier lowering remains unclear: The current-voltage (I-V) measurements are unable to discriminate between local intensification of electric field at the interface[8,9] and trap mediated tunneling,[3,9] as both the electric field strength (F) and the tunneling barrier height (Φ) enter the Fowler–Nordheim (FN) exponent together:[10,11] $I=aF^2\exp(-b\phi^{3/2}F^{-1})$. Therefore, we choose a different approach in the present work, i.e., photon stimulated tunneling (PST) of electrons into the BOX under laser excitation, which allowed us to extract Φ independently. The experiments reveal the presence of defects with energy level at 2.8 eV below the SiO_2 conduction band, of which the density is sensitive to the Si enrichment of the oxide. The unveiled correlation between the dark I-V curves and PST quantum yield points to the isolated defects as the source of the degraded BOX resistivity.

The samples studied were both commercial and experimentally processed SIMOX structures on (100)Si. Standard SIMOX was fabricated by implanting O^+ doses of $(1.7–1.8)\times10^{18}$ cm^{-2} in single (SI) or triple (TI) steps at 170–200 keV. The low-dose SIMOX material was produced by implanting 4×10^{17} cm^{-2} O^+/cm^2 at 120 or 180 keV. Post-implantation anneal was done at 1325–1350 °C in Ar $+0.5\%$ O_2 for 5–6 h. Some structures were subjected to additional treatments: supplemental implantation of 5×10^{17} O^+/cm^2 followed by a 1000 °C post-implantation anneal or internal thermal oxidation (ITOX) (1350 °C, Ar+30% O_2; 5 h). Finally, the top Si layers were replaced by semitransparent gold electrodes (13.5 nm thick) of 0.5 mm^2 area to form metal-oxide-semiconductor (MOS) structures. For the sake of comparison, the thermally grown oxides on (100)Si (1000 °C; O_2; 1.5 h) and deposited oxides on (100)Si (plasma assisted decomposition of silane at 500 °C) were studied as well. The oxide thickness was measured by single wavelength or spectroscopic ellipsometry.

The conductance of the BOX was studied by measuring the I-V curves under positive metal bias either in darkness or under irradiation by an Ar ion laser (Spectra Physics 168B). The latter provides nine spectral lines with the photon energy ($h\nu$) ranging from 2.41 to 2.73 eV, and an output power (P) of 25–200 mW. The photocurrent was measured as the difference between the dark current and the current under illumination. The relative quantum yield (Y) of the optically stimulated injection was determined in terms of photocurrent normalized to the incident light power. The strength of electric field was obtained from the applied bias potential, the metal-semiconductor work function difference as measured by electron photoinjection in the oxide, and the oxide thickness. All the measurements were performed at 300 K. The oxide charge was monitored using 1 MHz capacitance-voltage curves, indicating the density of trapped electrons to be below 2×10^{11} cm^{-2} in all the samples.

Typical FN plots of the dark current and photocurrents measured at three photon energies are shown in Fig. 1 for the MOS structures with the SI (a) and TI (b) SIMOX BOX. The samples show significant differences in the dark conductance: the low field quasi-ohmic conductance of the SI sample substantially exceeds that of the TI specimen, in agreement with the literature.[3] From the slope of the high field part of the dark FN curve the effective barrier height

[a]Electronic mail: valery.afanasiev@fys.kuleuven.ac.be

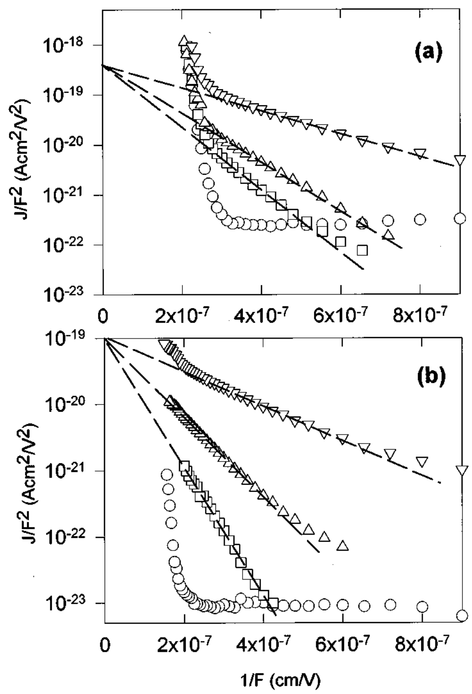

FIG. 1. Fowler–Nordheim plots of the dark (○) and the PST currents measured at photon energy 2.41 (□), 2.54 (△), and 2.71 eV (▽) in the MOS structures with SIMOX BOX produced by (a) single and (b) triple implantation. The PST currents are normalized to the incident light power of 1 W. The lines show the PST behavior expected from the FN model.

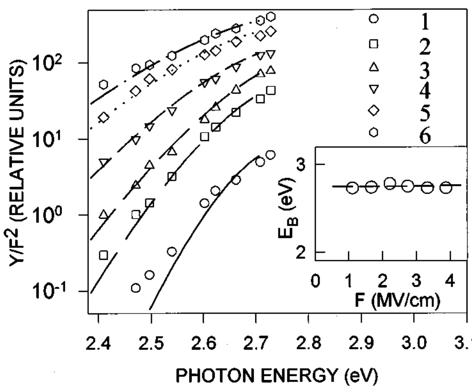

FIG. 2. Spectral dependences of the PST quantum yield in the SI SIMOX BOX taken at different strength of the electric field (in MV/cm): 1.1 (1), 1.67 (2), 2.22 (3), 2.75 (4), 3.33 (5), and 3.88 (6). The lines represent the FN model fitting results. The binding energy of the initial electron state of the PST transition E_B obtained from the fitting is shown in the insert as a function of electric field.

can be estimated as 1.4 and 1.7 eV for the SI and TI samples, respectively. The photocurrent shows the FN behavior, which suggests tunneling as the limiting process. In addition, the current density and the slope of the FN curve are sensitive to the photon energy indicating an optical transition to be involved in the rate limiting step as well. We found no dependence of the yield on the incident power for $P<0.5$ W, which besides indicating a first order process, also demonstrates the insignificance of possible sample heating. Thus, the photon stimulated tunnel transitions control the photocurrent. At the same time, the photocurrent in the SI sample is substantially higher than in the TI one, which means there is a higher density of electrons available for the tunnel transitions in the former case. This cannot be related to a difference in the substrate doping as both samples were made on the low-doped p-Si ($n_a-n_d\sim10^{15}$ cm^{-3}). Noteworthy is the increase of the photocurrent in the SI sample in registry with the increase of the dark current at high fields, as shown in Fig. 1(a). In the TI sample the PST curve measured at $h\nu=2.71$ eV shows similar behavior [cf. Fig. 1(b)]. Apparently, then, the density of electrons contributing to the PST transitions is sensitive to the particular BOX fabrication process and increases at high fields.

The simultaneous variation of the tunneling probability and the electron density obscures the I-V curve analysis within the framework of the simple FN model. Thus, in order to keep the electron density constant, we analyzed $Y(h\nu)$ dependences at a fixed oxide field. The results are shown in Fig. 2. Following the FN model,[10,11] the dependences of the PST yield on photon energy were fitted as $Y/F^2=A\exp[-6.83\times10^7(m_{ox}/m_0)^{1/2}\Phi^{3/2}F^{-1}]$, where A is a constant, $m_{ox}=0.5m_0$ is the electron effective mass in the oxide, m_0 the electron rest mass, and $\Phi=E_B-h\nu$ (E_B is the energy of the initial state of the electron measured relative to the SiO_2 conduction band). A and E_B are the adjustable parameters. The fitting results, shown as curves in Fig. 2, agree well with the experimental data. E_B is found field-independent in the range $F=1$–4 MV/cm as shown in the inset. A remarkable observation is that $E_B=2.77\pm0.05$ eV is the same for all studied MOS structures irrespective of the oxide type. Consequently, the FN exponent is identical for all the samples and there are no significant local variations of electric field strength.

In general, the pre-exponential factor A is proportional to the density of electrons available for tunneling.[10,11] Taking into account the E_B invariance, the field dependence of A may be calculated as $A(F)=(Y/F^2)\exp[6.83\times10^7(m_{ox}/m_0)^{1/2}(E_B-h\nu)^{3/2}F^{-1}]$ from the PST current-voltage (I-V) curves. The results obtained from the $h\nu=2.71$ eV curves for different samples are shown in Fig. 3. Relative to the commercial SI SIMOX, A is enhanced for the SI SIMOX BOX implanted in the channeling direction, but decreases in the case of off-channeling implantation, as shown in Fig. 3(a). Supplemental implantation of oxygen in the SI BOX results in substantial A decrease, suggesting elimination of the corresponding electron states by oxidation. In the TI and ITOX processed low-dose SIMOX BOX, the $A(F)$ curve approaches that of thermally grown SiO_2 [Fig. 3(b)]. The deposited sample behavior, by contrast, is closer to SI SIMOX BOX. Such strong sensitivity of the PST pre-exponential factor to the oxide processing, as born out here by Fig. 3, points to oxide defects as the initial states of electrons rather than to the accumulation/inversion layer of Si, as previously believed.[11] For comparison, the quantum yield of overbarrier photoemission into the oxide from Si remains constant in the same samples within an accuracy of 20%.

The samples studied here have been analyzed previously by electron trapping and photodepopulation measurements.[12–14] The spectrally resolved photodepopulation gave a binding energy of 2.8 eV for electrons trapped in the BOX [see Fig. 2(b) in Ref. 14], i.e., equal to E_B determined from the present PST spectra. The density of these electron

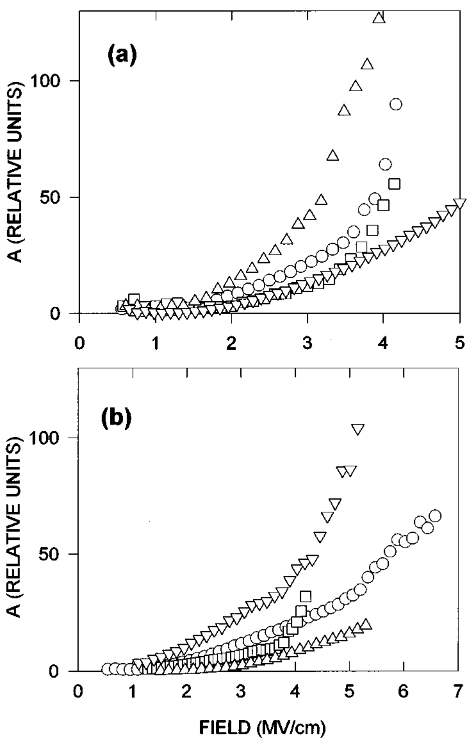

FIG. 3. Pre-exponential factor A for different samples vs electric field calculated from the PST I-V curves taken at $h\nu=2.71$ eV: (a) SI SIMOX samples: commercial (○), implanted in off-channeling (□) and in channeling (△) directions, and subjected to the supplemental implantation of oxygen into the BOX (▽); (b) TI SIMOX BOX (○), low dose SIMOX BOX subjected to ITOX (□), thermally grown (△), and deposited (▽) oxides.

traps increases in the case of in-channel implantation,[12] but decreases in the TI samples and after supplemental implantation of oxygen.[13] As the overbarrier photodepopulation is likely to sense the same type of defects as the subbarrier PST, the reliability of the energy level determination is assured. The $A(F)$ curves shown in Fig. 3 indicate that the filling of these electron states starts from $F \geqslant 2$ MV/cm onward. This allows a simple calculation of the defect location. Taking into account the conduction band offset of 3.15 eV at the (100)Si/SiO_2 interface[15] and using the fact that the position of the Si Fermi level is close to the first quantum subband at the (100)Si surface (0.1 eV above the Si conduction band edge[16]), it is easily deduced that E_B will cross the Fermi level at 2 MV/cm for the traps located at ~1.5 nm away from the Si surface. This location explains rapid refilling of the defects by electrons from Si, which is necessary to maintain the observed stable-in-time PST current.

A major observation regards the correlation between the dark conductivity and PST current of SiO_2 layers. The correlation is borne out in two ways. First, all the technological variations leading to the improvement of the BOX insulating properties (excess Si reduction by off-channel and multiple implantation, supplemental oxygen implantation, ITOX, reoxidation) were also found to reduce the density of the defects contributing to the PST. This would mean that the dark conductance and the PST are related to the defects of similar chemical origin (excess Si). Second, the dark conductance I-V curves of the SIMOX BOX repeatedly show a current increase from $F \geqslant 2$ MV/cm onward[3–6]—the very same behavior as exhibited by the $A(F)$ curves deduced from PST shown in Fig. 3. Thus, the *filling* of the same states with electrons gives rise both to the dark and the PST currents. The latter correlations indicate that the *same* defects control both conductance of BOX and the PST.

The observation of an electron state with identical binding energy in all oxides studied (SIMOX BOX, thermal, deposited) strongly suggests it to be related to an intrinsic defect in SiO_2. The decreasing defect density with reducing oxide Si enrichment would typify them as an excess Si center in SiO_2. The electron spin resonance experiments did not reveal dangling bond defects in the as-prepared oxides. But upon hole injection into the oxide, E'_γ centers are produced ($O_3 \equiv Si \cdot$ centers in SiO_2) with a particularly high density in SIMOX BOX,[17] which correlates at least qualitatively with the high density of the centers involved in PST in these oxides. However, it is unclear whether or not defects with identical atomic configuration may be responsible for both hole and electron trapping in SiO_2. In this context, a relationship of electron trapping with oxygen vacancy type defects has indeed been suggested for the thermally grown oxides[18] and Si^+ implanted oxides,[19] but no spectroscopic evidence for amphoteric behavior for such defects in SiO_2 is available so far.

In conclusion, we found the dark conductance of the buried oxide of SIMOX structures correlated with the yield of photon stimulated tunneling of electrons excited from defect states with the energy level 2.8 eV below the SiO_2 conduction band. The defects are initially neutral and diamagnetic; they are filled by electrons from silicon under action of an electric field. Their density correlates with the Si enrichment of the oxide. They probably serve as intermediate states for the trap assisted electron tunneling into SiO_2.

[1] J.-P. Colinge, *Silicon-on-Insulator Technology: Materials to VLSI* (Kluwer, Boston, 1991).
[2] G. A. Brown and A. G. Revesz, J. Electrochem. Soc. **139**, 309C (1992).
[3] A. G. Revesz, G. A. Brown, and H. L. Hughes, J. Electrochem. Soc. **140**, 3222 (1993).
[4] M. J. Anc and W. A. Krull, Microelectron. Eng. **28**, 407 (1995).
[5] R. E. Stahlbush, H. L. Hughes, and W. A. Krull, IEEE Trans. Nucl. Sci. **NS-40**, 1740 (1993).
[6] B. J. Mrstik, P. J. McMarr, H. L. Hughes, M. J. Anc, and W. A. Krull, Appl. Phys. Lett. **67**, 3283 (1995).
[7] K. Kawamura, T. Nakajima, I. Hamaguchi, T. Yano, Y. Nagatake, and M. Tachimori, in *Proceedings of the 1995 IEEE International SOI Conference* (IEEE, Tucson, 1995), p.156.
[8] S. P. Wainwright, C. Ngwa, S. Hall, and W. Eccleston, Microelectron. Eng. **22**, 399 (1993).
[9] J. U. Yoon, J. Nec, J.-H. Yap, and J. E. Chung, in *Proceedings of the 1995 IEEE International SOI Conference* (IEEE, Tucson, 1995), p. 146.
[10] E. H. Snow, Solid State Commun. **5**, 813 (1967).
[11] Z. A. Weinberg and A. Hartstein, J. Appl. Phys. **54**, 2517 (1983).
[12] V. V. Afanas'ev, G. A. Brown, H. L. Hughes, S. T. Liu, and A. G. Revesz, J. Electrochem. Soc. **143**, 347 (1996).
[13] V. V. Afanas'ev, A. G. Revesz, and H. L. Hughes, J. Electrochem. Soc. **143**, 695 (1996).
[14] V. V. Afanas'ev, A. G. Revesz, W. Jenkins, and H. L. Hughes, in *Proceedings of the 1995 IEEE International SOI Conference* (IEEE, Tucson, 1995), p. 102.
[15] M. Lenzlinger and E. H. Snow, J. Appl. Phys. **40**, 278 (1969).
[16] F. Stern, Phys. Rev. B **5**, 4891 (1972).
[17] A. Stesmans and K. Vanheusden, J. Appl. Phys. **76**, 1681 (1994).
[18] P. Balk, M. Aslam, and D. R. Young, Solid State Electron. **27**, 709 (1984).
[19] A. Kalnitsky, J. P. Ellul, E. H. Poindexter, P. J. Caplan, R. A. Lux, and A. R. Boothroyd, J. Appl. Phys. **67**, 7359 (1990).